

Antiferromagnetism in MnO—Calculation of Near-Neighbor Spin Correlation Functions for $T < T_N$ †

L. C. BARTEL

Sandia Laboratories, Albuquerque, New Mexico 87115

(Received 4 September 1969)

Taking into account the exchange-striction effects, the near-neighbor spin correlation functions of MnO are calculated for temperatures below the Néel temperature by using Green's-function techniques with a random-phase Tyablikov decoupling approximation. The resulting theoretical calculations are compared to some experimental results, and it is concluded that the lattice-distortion-induced biquadratic exchange effects are sufficient to explain the experimental data. The trigonal distortion and isotropic volume contraction parameters are found to be $j/J_2=0.019$ and $j_2/J_2=0.0021$, respectively. The observed anomalous behavior of the next-nearest-neighbor spin correlation function near the Néel temperature is theoretically explained.

I. INTRODUCTION

THE magnetic properties of antiferromagnetic MnO and α -MnS have been of experimental and theoretical interest. The neutron diffraction experiments¹ give evidence that the spin ordering is of the second kind.² It has been suggested that the magnetic properties of MnO can be explained by the presence of *intrinsic* biquadratic exchange terms arising from the superexchange in addition to the usual bilinear exchange terms in the usual Heisenberg Hamiltonian.³ However, *effective* biquadratic terms arise because of the balance setup between exchange and elastic forces.⁴⁻⁶ The x-ray experiments of Bean and Rodbell⁵ and Morosin⁷ show that MnO undergoes a trigonal lattice distortion below the Néel temperature T_N as well as an exchange-striction volume contraction. A molecular-field approximation (MFA) has been applied by Rodbell and Owen⁶ to explain the experimental results.

More recently the theoretical pictures of antiferromagnetic MnO and α -MnS have been clarified by Lines^{8,9} and Lines and Jones.^{10,11} They used a Green's-function (GF) method, in the random-phase approximation (RPA) with the Tyablikov decoupling approximation (TDA), to examine in detail the magnetic properties. They considered the trigonal distortion below T_N for MnO and biquadratic exchange terms for α -MnS. The experimental data (neutron diffraction,¹ x-ray,^{5,7} and NMR¹⁰) support the theory that the magnetization curve can be explained on the basis of induced biquadratic terms due to the lattice distortion without invoking the intrinsic biquadratic terms arising

from the superexchange mechanism. In this paper we shall consider MnO only, although the techniques are applicable to other magnetic systems, e.g., α -MnS, NiO, FeO, etc.

In Sec. II we shall present the theory for the trigonal distortion and isotropic volume contraction which are related to the nearest-neighbor (nn) and next-nearest-neighbor (nnn) spin correlation functions (SCF's), respectively. The effects of crystalline anisotropy and magnetostriction are believed to be small compared to the exchange energy¹⁰ at low temperatures and are therefore ignored; only the effects of the spatial dependence of the nn and nnn exchange constants (exchange striction) will be considered. In addition, we shall derive, relying heavily on previous work,⁸⁻¹⁰ the equations necessary to solve for the transverse spin correlation function (TSCF) $\langle S_j^- S_i^+ \rangle$ using a GF technique in the RPA and in the TDA where we shall use the double-time GF's as discussed by Zubarev.¹² We shall also derive a theorem which allows us to calculate the longitudinal spin correlation function (LSCF) $\langle S_i^z S_j^z \rangle$ in terms of the TSCF. We can then combine the TSCF and LSCF to obtain the SCF $\langle \mathbf{S}_i \cdot \mathbf{S}_j \rangle$. The calculations pertaining to MnO are presented, compared to experimental data, and discussed in Sec. III. The experimentally observed⁷ anomaly in the isotropic volume contraction in MnO at T_N is also discussed in terms of the theory.

II. THEORETICAL CONSIDERATIONS

For temperatures above T_N , MnO, as well as many other iron-group simple compounds, belongs to the fcc symmetry class of the NaCl lattice, and for temperatures below T_N , undergoes a trigonal distortion and an isotropic volume contraction.⁵⁻¹¹ The spin pattern for $T < T_N$ has been observed to be of the fcc type-2.^{1,2} For this spin pattern the nn spins are ferromagnetically aligned when they are on the same (111) sheet as the reference spin and antiferromagnetically aligned when they are on adjacent (111) sheets. The nnn spins are

¹² D. N. Zubarev, Usp. Fiz. Nauk **71**, 71 (1960) [English transl.: Soviet Phys.—Usp. **3**, 320 (1960)].

† Work supported by the U. S. Atomic Energy Commission.

¹ C. G. Shull, W. A. Strausser, and E. O. Wollan, Phys. Rev. **83**, 333 (1951).

² P. W. Anderson, Phys. Rev. **79**, 705 (1950).

³ D. S. Rodbell, I. S. Jacobs, J. Owen, and E. A. Harris, Phys. Rev. Letters **11**, 10 (1963).

⁴ C. Kittel, Phys. Rev. **120**, 335 (1960).

⁵ C. P. Bean and D. S. Rodbell, Phys. Rev. **126**, 104 (1962).

⁶ D. S. Rodbell and J. Owen, J. Appl. Phys. **35**, 1002 (1964).

⁷ B. Morosin, Phys. Rev. (to be published).

⁸ M. E. Lines, Phys. Rev. **135**, A1336 (1964).

⁹ M. E. Lines, Phys. Rev. **139**, A1304 (1965).

¹⁰ M. E. Lines and E. D. Jones, Phys. Rev. **139**, A1313 (1965).

¹¹ M. E. Lines and E. D. Jones, Phys. Rev. **141**, 525 (1966).

antiferromagnetically aligned and are on adjacent (111) sheets.

When there exists the trigonal distortion from the fcc NaCl structure below T_N , the resulting crystallographic symmetry of the unit cell would properly be described as rhombohedral with an angle α near 60° .⁷ In the previous studies, the pseudocubic cell (four times the volume of the primitive cell) has been found useful in the analysis.⁵⁻¹⁰ We shall use the pseudocubic cell in the following work.

Let the trigonally deformed cube have corner angles $\frac{1}{2}\pi \pm \Delta$. For small values of the distortion parameter Δ the distance d^+ between parallel pairs of nn spins and the distance d^- between antiparallel nn spins is given by Lines and Jones¹⁰ as

$$d^\pm = d(1 \pm \frac{1}{2}\Delta), \quad (1)$$

where d is the nn distance in the cubic phase. In addition, the nn distance will decrease owing to the isotropic lattice contraction $\delta a/a$. The exchange interaction between d^- neighbors (J_1^+) and between the d^+ neighbors (J_1^-) may be written^{10,11}

$$J_1^\pm = J_1(1 \pm \frac{1}{2}\epsilon_1\Delta - \epsilon_1\delta a/a), \quad (2)$$

where ϵ_1 and Δ are positive if exchange decreases with increasing spin separation. We also assume that the nnn spin interaction changes with nnn spin distance. The nnn exchange-coupling constant depends on the isotropic contraction of the lattice so that

$$J_2' = J_2(1 - \epsilon_2\delta a/a), \quad (3)$$

where ϵ_1 and ϵ_2 are given by

$$\epsilon_1 = -r\partial \ln J_1 / \partial r, \quad (4a)$$

$$\epsilon_2 = -r\partial \ln J_2 / \partial r. \quad (4b)$$

The spin Hamiltonian is taken to be¹⁰

$$\mathcal{H} = \sum_{nn} J_1^- \mathbf{S}_i \cdot \mathbf{S}_j + \sum_{nn} J_1^+ \mathbf{S}_i \cdot \mathbf{S}_j + \sum_{nnn} J_2' \mathbf{S}_i \cdot \mathbf{S}_j, \quad (5)$$

where \sum_{nn}^p and \sum_{nn}^a refer to summation over nn parallel and antiparallel spin pairs, respectively, and \sum_{nnn} refers to a summation over nnn spin pairs. In this work, J_1 and J_2 as they appear in Eqs. (2) and (3) are intrinsically positive.

The elastic free energy which includes the shear and isotropic contraction terms is written as^{6,10}

$$F_{el} = \frac{3}{2}C_{44}\Delta^2 + \frac{1}{2}\left(\frac{C_{11}+2C_{12}}{3}\right)\left(\frac{3\delta a}{a}\right)^2, \quad (6)$$

where C_{11} , C_{12} , and C_{44} are the usual elastic constants for cubic materials. Now $\partial F_{ex} / \partial \Delta = \langle \partial \mathcal{H} / \partial \Delta \rangle$ and similarly when the derivative is taken with respect to $\delta a/a$.¹⁰ The angular bracket denotes a thermal average over the ensemble. Thus minimizing the free energy

with respect to Δ and $\delta a/a$, we obtain for the equilibrium values of Δ and $\delta a/a$

$$\Delta_{eq} = z_1 N J_1 \epsilon_1 S^2 / 24C_{44}, \quad (7a)$$

$$S^2 = \langle \mathbf{S}_i \cdot \mathbf{S}_j \rangle_{nn}^p - \langle \mathbf{S}_i \cdot \mathbf{S}_j \rangle_{nn}^a, \quad (7b)$$

$$(\delta a/a)_{eq} = \frac{z_2 N J_2 \epsilon_2 \langle \mathbf{S}_i \cdot \mathbf{S}_j \rangle_{nnn} + \frac{1}{2} z_1 N J_1 \epsilon_1 \mathcal{R}^2}{6(C_{11} + 2C_{12})}, \quad (8a)$$

$$\mathcal{R}^2 = \langle \mathbf{S}_i \cdot \mathbf{S}_j \rangle_{nn}^p + \langle \mathbf{S}_i \cdot \mathbf{S}_j \rangle_{nn}^a, \quad (8b)$$

where N is the number of spins in the system, z_1 and z_2 are numbers of nn and nnn, respectively, and ϵ_1 and ϵ_2 are defined by Eqs. (4a) and (4b). In the MFA for $T < T_N$, $S^2 = 2(\bar{S})^2$ and $\mathcal{R}^2 = 0$, and for $T > T_N$, $S^2 = 0$ but $\mathcal{R}^2 \neq 0$. Using Δ_{eq} and $(\delta a/a)_{eq}$ given by Eqs. (7a) and (8a), the exchange constants J_1^\pm and J_2' in the Hamiltonian Eq. (5) become

$$J_1^\pm = J_1 \pm \frac{1}{2} j S^2 - (J_1 \epsilon_1 / J_2 \epsilon_2) j_2 \langle \mathbf{S}_i \cdot \mathbf{S}_j \rangle_{nnn} - \frac{1}{2} j' \mathcal{R}^2, \quad (9a)$$

$$J_2' = J_2 - j_2 \langle \mathbf{S}_i \cdot \mathbf{S}_j \rangle_{nnn} - \frac{1}{2} (J_2 \epsilon_2 / J_1 \epsilon_1) j' \mathcal{R}^2, \quad (9b)$$

where

$$j = z_1 N \epsilon_1^2 J_1^2 / 24C_{44}, \quad (10a)$$

$$j_2 = z_2 N \epsilon_2^2 J_2^2 / 6(C_{11} + 2C_{12}), \quad (10b)$$

$$j' = (z_1 J_1^2 \epsilon_1^2 / z_2 J_2^2 \epsilon_2^2) j_2. \quad (10c)$$

In the Appendix, we show an alternative method for obtaining the effective Hamiltonian given by Eq. (5) with the exchange constants given by Eqs. (9a)–(10c).

The GF's that need to be calculated can be calculated using Lines's^{8,9} techniques and results, where Lines used the double-time GF's as discussed by Zubarev.¹² The spin S is taken to obey the commutation relations

$$[S_i^+, S_j^-] = 2\delta_{ij} S_i^z, \quad (11a)$$

$$[S_i^+, S_j^z] = -S_i^+ \delta_{ij}, \quad (11a)$$

$$[S_i^-, S_j^z] = S_i^- \delta_{ij},$$

where

$$S_j^+ = S_j^x + iS_j^y, \quad S_j^- = S_j^x - iS_j^y. \quad (11b)$$

For spins i and j on the same sublattice we have from the work of Lines^{8,9}

$$\langle \langle S_i^+; B_j \rangle \rangle = (2/N) \sum_{\mathbf{K}} G_{1\mathbf{K}} e^{i\mathbf{K} \cdot (i-j)}, \quad (12a)$$

$$G_{1\mathbf{K}} = \sum_{i-j} \langle \langle S_i^+; B_j \rangle \rangle e^{-i\mathbf{K} \cdot (i-j)}, \quad (12b)$$

$$B_j = f(S_j^z) S_j^-, \quad (12c)$$

where N is the total number of spins in the lattice, and where \mathbf{K} is a reciprocal vector which runs over $\frac{1}{2}N$ points in the first Brillouin zone of the reciprocal sublattice.⁸ In a similar manner, $G_{2\mathbf{K}}$ is defined for spins

i and j on different sublattices. The resulting GF's are^{8,9}

$$G_{1\mathbf{K}} = \frac{F}{4\pi} \left[\frac{1-A}{E+\bar{S}E_0} + \frac{1+A}{E-\bar{S}E_0} \right], \quad (13a)$$

$$G_{2\mathbf{K}} = -\frac{F}{4\pi} \left[\frac{-C}{E+\bar{S}E_0} + \frac{C}{E-\bar{S}E_0} \right], \quad (13b)$$

where $A = \mu/E_0$, $C = \lambda/E_0$, $E_0 = (\mu^2 - \lambda^2)^{1/2}$, \bar{S} is the average spin per magnetic atom, and $F = \langle [S_i^+, B_i] \rangle$. The quantities μ and λ are defined by⁸⁻¹⁰

$$\begin{aligned} \mu + \lambda = & 4J_1'(c_1c_2 + c_2c_3 + c_3c_1) + 4J_2[1 - (j_2/J_2) \\ & \times \langle \mathbf{S}_i \cdot \mathbf{S}_j \rangle_{\text{nnn}}] (c_1^2 + c_2^2 + c_3^2) + 4j(\frac{1}{2}S^2) \\ & \times (3 - s_1s_2 - s_2s_3 - s_3s_1), \end{aligned} \quad (14a)$$

$$\begin{aligned} \mu - \lambda = & 4J_1'(s_1s_2 + s_2s_3 + s_3s_1) + 4J_2[1 - (j_2/J_2) \\ & \times \langle \mathbf{S}_i \cdot \mathbf{S}_j \rangle_{\text{nnn}}] (s_1^2 + s_2^2 + s_3^2) + 4j(\frac{1}{2}S^2) \\ & \times (3 - c_1c_2 - c_2c_3 - c_3c_1), \end{aligned} \quad (14b)$$

$$J_1' = J_1 - (J_1 \epsilon_1 j_2 / J_2 \epsilon_2) \langle \mathbf{S}_i \cdot \mathbf{S}_j \rangle_{\text{nnn}} - \frac{1}{2} j' \mathcal{R}^2, \quad (14c)$$

where $c_l = \cos K_l a$, $s_l = \sin K_l a$, and $l = x, y, z$.

The CF $\langle B_j S_i^+ \rangle$ is calculated from^{8,12}

$$\begin{aligned} \langle B_j S_i^+ \rangle = & \lim_{\epsilon \rightarrow 0} i \int_{-\infty}^{\infty} dE \\ & \times \frac{\langle \langle S_i^+; B_j \rangle \rangle_{E+i\epsilon} - \langle \langle S_i^+; B_j \rangle \rangle_{E-i\epsilon}}{e^{E/kT} - 1}, \end{aligned} \quad (15a)$$

where

$$\begin{aligned} \lim_{\epsilon \rightarrow 0} \left(\frac{1}{E+i\epsilon - E_{\mathbf{K}}} - \frac{1}{E-i\epsilon - E_{\mathbf{K}}} \right) \\ = -2\pi i \delta(E - E_{\mathbf{K}}). \end{aligned} \quad (15b)$$

Therefore, from Eqs. (11a)-(15b) for $f(S_j^z) = 1$ when i and j are on the same sublattice we have

$$\langle S_j^- S_i^+ \rangle = \frac{1}{2} F \langle e^{i\mathbf{K} \cdot (i-j)} [A \coth(\bar{S}E_0/2kT) - 1] \rangle_{\mathbf{K}}, \quad (16a)$$

and when i and j are on different sublattices

$$\langle S_j^- S_i^+ \rangle = -\frac{1}{2} F \langle e^{i\mathbf{K} \cdot (i-j)} C \coth(\bar{S}E_0/2kT) \rangle_{\mathbf{K}}, \quad (16b)$$

where here $F = 2\bar{S}$. The brackets $\langle \dots \rangle_{\mathbf{K}} = (2/N) \times \sum_{\mathbf{K}} (\dots)$ where again \mathbf{K} runs over $\frac{1}{2}N$ values in the first Brillouin zone of the reciprocal lattice.

In calculating the SCF's $\langle \mathbf{S}_i \cdot \mathbf{S}_j \rangle$, we can write this as

$$\langle \mathbf{S}_i \cdot \mathbf{S}_j \rangle = \langle S_j^- S_i^+ \rangle + \langle S_i^z S_j^z \rangle \quad \text{for } i \neq j. \quad (17)$$

The TSCF $\langle S_j^- S_i^+ \rangle$ is relatively simple to calculate using standard GF techniques. However, the LSCF $\langle S_i^z S_j^z \rangle$ is somewhat difficult to calculate. A spectral theorem similar to the one introduced by Mills¹³ can be used to calculate the LSCF in terms of the TSCF. In what follows we shall derive this theorem in a more

usable form, namely, in terms of the GF rather than the spectral function. We shall then use this theorem to evaluate the SCF's [Eq. (17)] for nn parallel and anti-parallel spins and for nnn spins.

The average spin per site \bar{S} can be calculated from Lines⁸ expression

$$\frac{2\bar{S} + x}{2S + 1} = \frac{(x+1)^{2S+1} + (x-1)^{2S+1}}{(x+1)^{2S+1} - (x-1)^{2S+1}}, \quad (18a)$$

$$x = \langle A \coth(\bar{S}E_0/2kT) \rangle_{\mathbf{K}}, \quad (18b)$$

where the transcendental equation [Eq. (18a)] is to be solved for \bar{S} .

Mills¹³ has given a proof that the expectation value of the Heisenberg exchange Hamiltonian for ferromagnetism could be computed, knowing only the TSCF's. We shall now prove the theorem for general operators $A(t)$ and $B(t')$ ($t \neq t'$ in general) using the spectral representation function as is usually defined so that the formalism discussed by Zubarev¹² can be used. The advantage of the form of the theorem we shall derive is that it can be expressed in terms of the Green's function as well as in terms of the spectral representation function. The theorem can be derived in a straightforward manner from Zubarev's paper. Combining Zubarev's Eqs. (3.7a) and (3.7b), expressing the spectral function in terms of the advanced and retarded GF's [Eq. (3.25)], and differentiating n times with respect to t' , we have for the n th moment theorem

$$\begin{aligned} \lim_{\epsilon \rightarrow 0} (-i)\eta \int_{-\infty}^{\infty} dE E^n e^{-iE(t-t')} \\ \times [\langle \langle A; B \rangle \rangle_{E+i\epsilon} - \langle \langle A; B \rangle \rangle_{E-i\epsilon}] \\ = \langle [[\mathcal{I}C, [\mathcal{I}C, \dots [\mathcal{I}C, [\mathcal{I}C, B(t')]_-]_- \dots]_-]_-, A(t) \rangle \rangle, \end{aligned} \quad (19)$$

where the expression on the left-hand side of the commutator, whose right-hand member is $A(t)$, represents n nested commutators, $i[\mathcal{I}C, B(t')]_-$ is the time derivative operator, and $[A, B] = AB - \eta BA$ where $\eta = \pm 1$. We are using the units $\hbar = 1$.

We now consider the GF $\langle \langle S_i^+; S_j^- \rangle \rangle_E$ and $\mathcal{I}C$ to be given by Eq. (5). At equal times for $n=0$ we find that the application of Eq. (19) gives an identity indicating the decoupling scheme is a proper one. For $n=1$ we arrive at an expression for the LCF in terms of the TCF as we will show below.

Applying Eq. (19) for $n=1$ and using Eqs. (5), (16a)-(17) we have for $i \neq j$ but i and j on the same sublattice

$$\begin{aligned} \langle [[\mathcal{I}C, S_j^-]_-, S_i^+]_- \rangle = & -J_1^- [\langle S_j^- S_i^+ \rangle + 2\langle S_i^z S_j^z \rangle] \\ = & -[4(\bar{S})^2/N] \sum_{\mathbf{K}} e^{i\mathbf{K} \cdot (i-j)\mu} \\ = & -2(\bar{S})^2 J_1^-, \end{aligned} \quad (20)$$

¹³ R. E. Mills, Phys. Rev. Letters 18, 1189 (1967).

and for $i \neq j$ and i and j on different sublattices we have

$$\begin{aligned} & \langle [[\mathcal{H}C, S_j^-]_-, S_i^+]_- \rangle \\ &= - \left\{ \begin{array}{l} J_1^+ \text{ for } i \text{ and } j \text{ nn} \\ J_2' \text{ for } i \text{ and } j \text{ nnn} \end{array} \right\} [\langle S_j^- S_i^+ \rangle + 2 \langle S_i^z S_j^z \rangle] \\ &= (4/N) (\bar{S})^2 \sum_{\mathbf{K}} e^{i\mathbf{K} \cdot (i-j)\lambda} \\ &= 2(\bar{S})^2 \left\{ \begin{array}{l} J_1^+ \\ J_2' \end{array} \right\}. \end{aligned} \quad (21)$$

Solving for $\langle S_i^z S_j^z \rangle$ when $i \neq j$ from Eqs. (20) and (21), we have from Eq. (17) for i and j on the same sublattice

$$\begin{aligned} \langle \mathbf{S}_i \cdot \mathbf{S}_j \rangle &= (\bar{S})^2 + \frac{1}{2} \langle S_j^- S_i^+ \rangle \\ &= (\bar{S})^2 + \frac{1}{2} \bar{S} \langle e^{i\mathbf{K} \cdot (i-j)} A \coth \bar{S} E_0 / 2kT \rangle_{\mathbf{K}}, \end{aligned} \quad (22a)$$

and for i and j on different sublattices we have

$$\begin{aligned} \langle \mathbf{S}_i \cdot \mathbf{S}_j \rangle &= -(\bar{S})^2 + \frac{1}{2} \langle S_j^- S_i^+ \rangle \\ &= -(\bar{S})^2 - \frac{1}{2} \bar{S} \langle e^{i\mathbf{K} \cdot (i-j)} C \coth \bar{S} E_0 / 2kT \rangle_{\mathbf{K}}. \end{aligned} \quad (22b)$$

The CF $\langle \mathbf{S}_i \cdot \mathbf{S}_j \rangle_{\text{nn}}^p$ is found from Eq. (22a), and the SCF's $\langle \mathbf{S}_i \cdot \mathbf{S}_j \rangle_{\text{nn}}^a$ and $\langle \mathbf{S}_i \cdot \mathbf{S}_j \rangle_{\text{nnn}}$ are found from Eq. (22b).

At this point it should be noted that the theorem given by Eq. (19) is an exact statement which depends on knowing the exact GF. However, as Eq. (19) was applied to obtain Eqs. (22a) and (22b), the GF was obtained through an RPA with a particular decoupling scheme, and the accuracy of the results for the SCF's depends on the TDA as well as the RPA. As will be shown in Sec. III, the agreement between the theoretically calculated and experimentally determined SCF's is remarkable, indicating the RPA with the TDA are good approximations for this problem.

When T approaches T_N from below $\bar{S} \rightarrow 0$ and from Eqs. (20) and (21) it is obvious that $\langle S_i^z S_j^z \rangle |_{T_N^-} = -\frac{1}{2} \langle S_j^- S_i^+ \rangle |_{T_N^-}$, where the TSCF's can be calculated from Eqs. (16a) and (16b) in the limit of $\bar{S} \rightarrow 0$. When $i \neq j$, we have for i and j on the same sublattice

$$\langle S_j^- S_i^+ \rangle |_{T_N^-} = 2kT_N \langle e^{i\mathbf{K} \cdot (i-j)} A / E_0 \rangle_{\mathbf{K}}, \quad (23a)$$

and for i and j on different sublattices we have

$$\langle S_j^- S_i^+ \rangle |_{T_N^-} = -2kT_N \langle e^{i\mathbf{K} \cdot (i-j)} C / E_0 \rangle_{\mathbf{K}}. \quad (23b)$$

These results [Eqs. (23a) and (23b)] agree with Lines' results for $T \rightarrow T_N^-$ [Eqs. (4.37) and (4.38) of Ref. 8 where the yy SCF $\langle S^y S^y \rangle$ has a value of $\frac{1}{2} \langle S^- S^+ \rangle$ and kT_N is given by Eq. (2.26) of Ref. 8]. Now since the xx and yy SCF's are equal, we have from Eqs. (17), (20), (21), (23a), (23b) that for $T \rightarrow T_N$ from below, the zz SCF is equal in magnitude to the xx and yy SCF's but has opposite sign. However, for $T \rightarrow T_N$ from above, the xx , yy , and zz SCF's are all equal and have the same sign, indicating an anomalous behavior of the $\langle \mathbf{S}_i \cdot \mathbf{S}_j \rangle$ SCF at the ordering temperature. We shall discuss this result in Sec. III.

III. CALCULATIONS AND DISCUSSION

In this section we calculate the nn and nnn SCF's for MnO using the equations developed in Sec. II. The parameters to be used in the calculation of the SCF's are determined from the available experimental data. The procedure for the calculation of j [Eq. (10a)] and j_2 [Eq. (10b)] is as follows. It is apparent from Eqs. (7a) and (8) that the evaluation of j and j_2 from the trigonal distortion and isotropic volume contraction data requires knowing the SCF's, which in turn requires knowledge of these parameters. Thus we must use a bootstrap technique to obtain values for these parameters. Using a value of $\bar{S} = 2.43$ (where the spin $S = \frac{5}{2}$ for the Mn^{2+} ion in MnO at $T = 0^\circ\text{K}$)¹⁰ we replaced $\frac{1}{2} s^2$ by $(\bar{S})^2$ and $\langle \mathbf{S}_i \cdot \mathbf{S}_j \rangle_{\text{nnn}}$ by $-(\bar{S})^2$ in Eqs. (7a) and (8a) and let $\mathcal{R}^2 = 0$. Then using the experimentally determined⁷ $\Delta_{\text{eq}} = 1.1 \times 10^{-2}$ and $(\delta a/a)_{\text{eq}} = 1.1 \times 10^{-3}$, we obtained values $J_{1\epsilon_1} = 230^\circ\text{K}$ and $J_{2\epsilon_2} = 130^\circ\text{K}$ where we used $N = 4.7 \times 10^{22} \text{ cm}^{-3}$ (Ref. 6), $C_{11} = 2.23 \times 10^{12} \text{ dyn cm}^{-2}$, $C_{12} = 1.2 \times 10^{12} \text{ dyn cm}^{-2}$, and $C_{44} = 0.79 \times 10^{17} \text{ dyn cm}^{-2}$,¹⁴ and $z_1 = 12$, and $z_2 = 6$. From Eqs. (10a) and (10b) we obtained the values $j/J_2 = 0.019$ and $j_2/J_2 = 0.0021$ where we used $J_1 = 10^\circ\text{K}$ and $J_2 = 11^\circ\text{K}$ as determined by Lines and Jones¹⁰ from the experimental data. We could then calculate $\frac{1}{2} s^2$, $\frac{1}{2} \mathcal{R}^2$, and $\langle \mathbf{S}_i \cdot \mathbf{S}_j \rangle_{\text{nnn}}$ to use in Eqs. (7a) and (8a) and then repeat the process. However, we found that using $\frac{1}{2} s^2 = (\bar{S})^2$, $\mathcal{R}^2 = 0$, and $\langle \mathbf{S}_i \cdot \mathbf{S}_j \rangle_{\text{nnn}} = -(\bar{S})^2$ in Eqs. (7a) and (8a) gave us satisfactory results for j/J_2 and j_2/J_2 . Note that our value of j/J_2 is approximately twice as large as the value Lines and Jones¹⁰ calculated for MnO, although our $J_{1\epsilon_1}$ agrees with their value. The reason for this is that their effective Hamiltonian found from the total free energy gives values for the distortion and isotropic volume contraction parameters one-half of our values. (For a discussion of their effective Hamiltonian, see the Appendix and Ref. 11.)

It is apparent from Eqs. (14a), (14b), (18a), (18b), (22a), and (22b) that the quantities \bar{S} , $\langle \mathbf{S}_i \cdot \mathbf{S}_j \rangle_{\text{nn}}^p$, $\langle \mathbf{S}_i \cdot \mathbf{S}_j \rangle_{\text{nn}}^a$, and $\langle \mathbf{S}_i \cdot \mathbf{S}_j \rangle_{\text{nnn}}$ are all interrelated, and the equations should be solved simultaneously for these quantities. However, the following procedure was used to solve for the above quantities. In solving for \bar{S} from Eq. (18a), we took $s^2 = 2(\bar{S})^2$, $\mathcal{R}^2 = 0$, and $\langle \bar{S}_i \cdot \bar{S}_j \rangle_{\text{nnn}} = -(\bar{S})^2$ in the expressions for $\mu + \lambda$ and $\mu - \lambda$ [Eqs. (14a) and (14b)]. The resulting \bar{S} was used to calculate the SCF's in the above approximation. For small values of j/J_2 and j_2/J_2 , we found that the error in the resulting SCF's from using this approximation was small. The method we used for calculating the sums is outlined below.

In calculating the sums over the Brillouin zone, the singular points, when $E_0 \rightarrow 0$, need special attention. The points in the sum over the first Brillouin zone where $E_0 \rightarrow 0$ were replaced by an integral around

¹⁴ D. W. Oliver, J. Appl. Phys. **40**, 893 (1969);

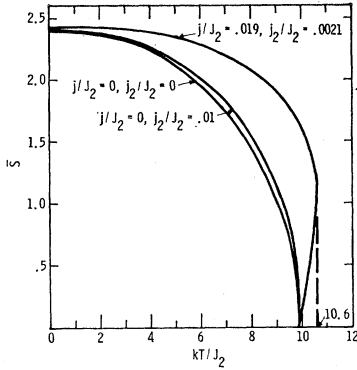


FIG. 1. Shown are curves of the average spin per site as a function of temperature which were calculated in the random-phase GF approximation for $S=\frac{5}{2}$, for $J_2/J_1=1.1$, and for various values of the trigonal distortion and isotropic volume contraction parameters.

these points. The points outside the integrated regions were summed in a conventional manner. The \mathbf{K} values ranged from $-\pi/a$ to π/a ,^{9,10} and a mesh of $(48)^3$ points was used.

We determined that for the above number of mesh points, the resulting SCF's did not change appreciably from calculations using meshes of $(24)^3$ and $(36)^3$. Because of the great expense of computer time and the small increase in accuracy in the SCF's, we did not feel that taking more mesh points was warranted.

In our calculations we used the ratio $J_2/J_1=1.1$, whereas Lines and Jones¹⁰ used $J_2/J_1=1.0$ for their calculations of \bar{S} for $T < T_N$. However, using the correct J_2/J_1 ratio did not greatly alter the \bar{S} -versus-temperature curve from their results.

To determine the effect of the isotropic volume contraction and the trigonal distortion on the shapes of

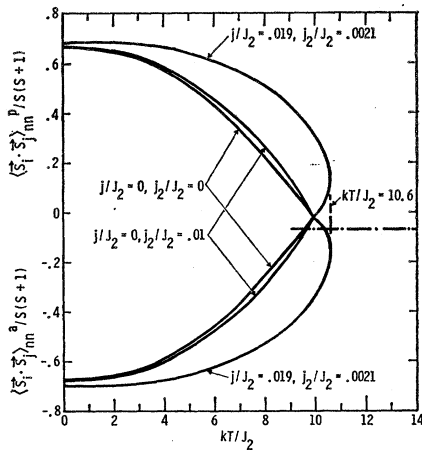


FIG. 2. The solid curves are the nn SCF's for parallel and anti-parallel aligned spins as functions of temperature which were calculated in the random-phase GF approximation for $S=\frac{5}{2}$, for $J_2/J_1=1.1$, and for various values of the trigonal distortion and isotropic volume contraction parameters. The dot-dashed curve is Lines's (Ref. 9) calculations for $T > T_N$, for $S=\frac{5}{2}$, and for $J_2/J_1=1$.

the average spin per site curve (\bar{S}) and the near-neighbor SCF curves, various values of j/J_2 and j_2/J_2 were used in the calculation of \bar{S} , $\langle \mathbf{S}_i \cdot \mathbf{S}_j \rangle_{nn} / S(S+1)$ and $\langle \mathbf{S}_i \cdot \mathbf{S}_j \rangle_{nnn} / S(S+1)$, and $\langle \mathbf{S}_i \cdot \mathbf{S}_j \rangle_{nnn} / S(S+1)$ versus kT/J_2 where $S=\frac{5}{2}$. The results are shown in Figs. 1-3. In addition, we calculated curves for $j/J_2=0$, $j_2/J_2=0.0021$ and $j/J_2=0.019$, $j_2/J_2=0$ and found that these curves *did not* differ significantly from the curves $j/J_2=0$, $j_2/J_2=0$ and $j/J_2=0.019$, $j_2/J_2=0.0021$, respectively.¹⁵ This indicates that the shapes of the \bar{S} and SCF curves versus temperature are rather insensitive to the isotropic volume contraction in agreement with the conclusions of Sievers and Tinkham.¹⁶ However, from the curves in Figs. 1-3 and from the work of Lines and Jones,¹⁰ it is clear that the shapes of the \bar{S} and of the SCF curves versus temperature are quite dependent on the amount of trigonal distortion, but the sensitivity to the trigonal distortion is diminished for values of $j/J_2 > 0.01$.¹⁰

When $j/J_2=0.019$, the \bar{S} and SCF curves are double valued for temperatures near the ordering temperature, indicating a first-order phase transition. That is, for a sufficient amount of trigonal distortion, the normal second-order phase transition (\bar{S} versus kT/J_2 for $j/J_2=0$ curve) is forced into a first-order phase

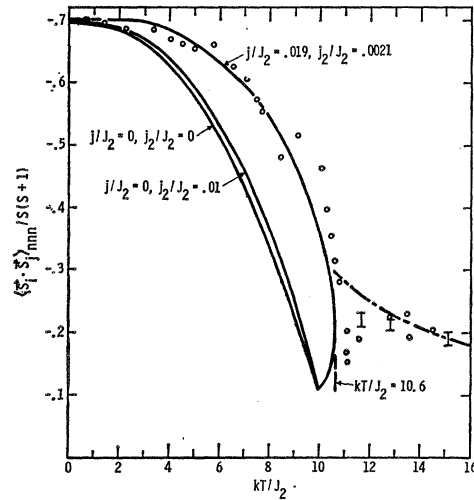


FIG. 3. The solid curves are the nnn SCF's as a function of temperature which were calculated in the random-phase GF approximation for $S=\frac{5}{2}$, for $J_2/J_1=1.1$, and for various values of the trigonal distortion and isotropic volume contraction parameters. The dot-dashed curve is Lines and Jones's (Ref. 10) calculations for $T > T_N$, for $S=\frac{5}{2}$, and for $J_2/J_1=1.1$. The open circles are Morosin's (Ref. 7) experimentally determined values for the correlation function, Eq. (8a), as a function of temperature, which were normalized to the $j/J_2=0.019$, $j_2/J_2=0.0021$ theoretical curve at $T=0^\circ\text{K}$. The straight vertical lines are Blech and Averbach's (Ref. 19) data.

¹⁵ At $T=0^\circ\text{K}$ there was *no* effect of $j_2/J_2=0, 0.0021$ on the $j/J_2=0, 0.019$ curves, while at higher temperatures the $j_2/J_2=0.0021$ curve was approximately a linewidth, Figs. 1-3, above the $j_2/J_2=0$ curves for $j/J_2=0, 0.019$.

¹⁶ A. J. Sievers, III, and M. Tinkham, Phys. Rev. **129**, 1566 (1963).

transition. Lines and Jones¹⁰ determined in their calculations that the transition from second to first order occurred for a distortion parameter of $0.001 < j/J_2 < 0.005$. For the first-order antiferromagnetic-to-paramagnetic phase transition we shall take the Néel temperature to be the largest temperature for which there is a solution; i.e., the right-hand extremity of the \bar{S} and of the SCF-versus- kT/J_2 curves for $j/J_2=0.019$, $j_2/J_2=0.0021$ of Figs. 1-3. Hence, we find that $kT_N/J_2=10.6$ and for $J_2=11^\circ\text{K}$ we have $T_N=117^\circ\text{K}$, which is in excellent agreement with the experimentally observed T_N of $117\pm 1^\circ\text{K}$.^{17,18}

The near-neighbor SCF's can be experimentally determined from the trigonal distortion and isotropic volume contraction data. Measurements of Δ_{eq} and $(\delta a/a)_{\text{eq}}$ give us measurements of $\langle \mathbf{S}_i \cdot \mathbf{S}_j \rangle_{\text{nn}}^p - \langle \mathbf{S}_i \cdot \mathbf{S}_j \rangle_{\text{nn}}^a$ and $\langle \mathbf{S}_i \cdot \mathbf{S}_j \rangle_{\text{nnn}}$ through Eqs. (7a) and (8a), respectively, where we set $\mathcal{R}^2=0$.

In order to determine $(\delta a/a)_{\text{eq}}$ experimentally, we must know the thermal expansion of the solid when there is no contribution from the magnetic interactions. Morosin⁷ has calculated the lattice constants for the "nonmagnetic" solid, and from his work we have $(\delta a/a)_{\text{eq}}$ versus temperature. In Fig. 3 we have plotted Morosin's⁷ data of $(\delta a/a)_{\text{eq}}(T)/(\delta a/a)_{\text{eq}}(T=0)$ normalized to the theoretical curve $j/J_2=0.019$, $j_2/J_2=0.0021$ at $T=0^\circ\text{K}$. (Calculation of j and j_2 from the data implies the normalization at $T=0^\circ\text{K}$.) For a comparison we have plotted in Fig. 3 the values of $\langle \mathbf{S}_i \cdot \mathbf{S}_j \rangle_{\text{nnn}}/S(S+1)$ for $T > T_N$ calculated by Lines and Jones¹⁰ for $J_2/J_1=1.1$. In their calculations they ignored the volume dependence of J_2 for $T > T_N$ which introduces a small but probably negligible error. In addition, we have plotted the diffuse neutron-scattering data of Blech and Averbach¹⁹ as given by Lines and Jones.¹⁰

In Fig. 4 we have plotted the theoretical curve of $(s^2/2)^{1/2}$ versus kT/J_2 obtained from Eq. (7b) and Fig. 2 for $j/J_2=0.019$ and $j_2/J_2=0.0021$. In addition, we have plotted Morosin's⁷ experimentally determined trigonal distortion data $[\Delta_{\text{eq}}(T)/\Delta_{\text{eq}}(T=0)]^{1/2}$ which were normalized to the theoretical $(s^2/2)^{1/2}$ curve at $T=0^\circ\text{K}$.

From Figs. 3 and 4 we see that there is excellent agreement between theory and experiment, and that the introduction of *intrinsic* biquadratic exchange terms are not needed to explain the experimental results. In Fig. 3 the predicted anomaly in the SCF at T_N (see Sec. II) is experimentally observed and has a magnitude of approximately the predicted value. The experimental points of Morosin⁷ in Fig. 3 show a marked departure from Lines and Jones's¹⁰ calculated curve just above T_N . At the higher temperatures, the experimental points fall approximately on the calculated

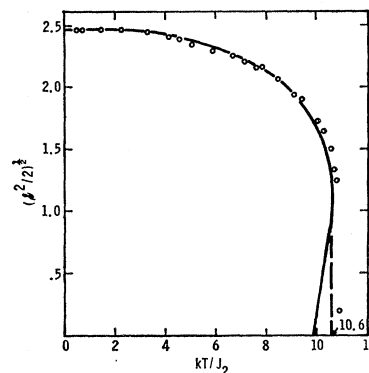


FIG. 4. The solid curve is the calculated curve of $(\frac{1}{2}s^2)^{1/2}$ as a function of temperature determined from Eq. (7b) and Fig. 2 for $j/J_2=0.019$ and $j_2/J_2=0.0021$. The open circles are Morosin's (Ref. 7) data of the trigonal distortion, $[\Delta_{\text{eq}}(T)/\Delta_{\text{eq}}(T=0)]^{1/2}$, normalized to the theoretical curve at $T=0^\circ\text{K}$.

curve. Note that Blech and Averbach's¹⁹ data show the same sort of departure from Lines and Jones's curve just above T_N as does Morosin's data. In Fig. 4 the agreement between the calculated curve and the experimental points is very good except for temperatures near T_N . Morosin's data give a T_N of 120°K , whereas the theoretical curve has $T_N=117^\circ\text{K}$.

The small discrepancies between the theory and experiment at T_N may be caused by (i) in the calculations, using J_2/J_1 and/or j/J_2 ratios which are too small; (ii) the possibility of an error in the measurement of the temperature in the experimental data (the experimental Δ_{eq} vanishes at a measured $T=120^\circ\text{K}$ rather than the expected $117\pm 1^\circ\text{K}$); (iii) the breakdown of the RPA with the TDA which were used in the calculations; (iv) the contribution to the lattice contraction because of a nonzero \mathcal{R}^2 for $T > T_N$; (v) the possibility of a nonzero s^2 just above T_N . Lines and Jones have ruled out this last possibility.¹⁰

It is interesting that MnO should be quite markedly a first-order phase transition with a respectable sized hysteresis. It is somewhat surprising that a large hysteresis and/or associated latent heat has so far escaped detection. Morosin²⁰ did, however, find a *small* amount of hysteresis in his work.

In order to resolve the discrepancies between the theoretical calculations and the experimental data for temperatures near T_N , it is hoped that the theoretical calculations and the predicted anomaly given in this paper will stimulate further experimental and theoretical investigations for temperatures near the ordering temperatures in magnetic systems—in particular, investigations into those systems which obey a Heisenberg-type model. In their calculations of the LSCF of the Heisenberg ferromagnetic, Tahir-Kheli and Callen²¹ have observed a difference between the TSCF and

¹⁷ R. W. Millar, J. Am. Chem. Soc. **50**, 1875 (1928).

¹⁸ S. S. Todd and K. R. Bonnickson, J. Am. Chem. Soc. **73**, 3894 (1951).

¹⁹ I. A. Blech and B. L. Averbach, Physics **1**, 31 (1964).

²⁰ B. Morosin (private communication).

²¹ R. A. Tahir-Kheli and H. B. Callen, Phys. Rev. **135**, A679 (1964).

LSCF for near-neighbor spins at the ordering temperature. A preliminary investigation shows that in a simple RPA GF calculation, the Ising model does not exhibit the anomaly for the nn SCF at the ordering temperature.

ACKNOWLEDGMENTS

The author wishes to acknowledge Dr. M. E. Lines and Dr. E. D. Jones for their helpful discussions about the problem. The author also wishes to acknowledge Dr. B. Morosin for suggesting the problem and for the many helpful discussions concerning the experimental data.

APPENDIX

It is the purpose of this Appendix to illustrate an alternative method for obtaining the effective spin-lattice coupled Hamiltonian used in Sec. II. To illustrate the method we shall consider the simplified Hamiltonian

$$\mathcal{H} = \mathbf{A} + \lambda \Delta \mathbf{A} + P^2/2\rho + \frac{1}{2}C\Delta^2, \quad (\text{A1})$$

where \mathbf{A} is a spin operator (e.g., $\sim \mathbf{S}_i \cdot \mathbf{S}_j$), Δ the lattice strain with the canonical momentum P , ρ is the density, C the appropriate elastic constant, and λ is the coupling constant. We can eliminate the interaction term (term linear in Δ) by a change in the origin. Let $\Delta = \Delta' - \Delta_0$ and choose Δ_0 to eliminate the terms linear in Δ' . The resulting Hamiltonian is

$$\mathcal{H} = \mathbf{A} - (\lambda^2/2C)\mathbf{A}^2 + P^2/2\rho + \frac{1}{2}C\Delta'^2, \quad (\text{A2})$$

which contains terms depending only on the spins (\mathbf{A} operator) and terms depending only on the lattice. In calculating the GF $\langle\langle S; B \rangle\rangle$ where S and B are some spin operators (suppressing sub- and superscripts), we have from the term quadratic in \mathbf{A} the GF

$$\langle\langle [S, \mathbf{A}] \mathbf{A} + \mathbf{A} [S, \mathbf{A}]; B \rangle\rangle$$

which we decouple as follows:

$$\langle\langle [S, \mathbf{A}] \mathbf{A} + \mathbf{A} [S, \mathbf{A}]; B \rangle\rangle \rightarrow 2\langle\mathbf{A}\rangle \langle\langle [S, \mathbf{A}]; B \rangle\rangle.$$

This decoupling scheme is equivalent to taking an effective Hamiltonian for the spin terms of

$$\mathcal{H}_s = \mathbf{A} - j\langle\mathbf{A}\rangle \mathbf{A}, \quad (\text{A3})$$

$$j = \lambda^2/C. \quad (\text{A4})$$

The effective Hamiltonian [Eqs. (A3) and (A4)] is equal to an effective Hamiltonian obtained by the method employed in Sec. II. That is, the effective Hamiltonian found by minimizing the free energy obtained from Eq. (A1) with respect to the lattice strain Δ , and then replaced Δ by its equilibrium value Δ_{eq} in the second term of Eq. (A1). This results in a spin Hamiltonian equal to \mathcal{H}_s given by Eqs. (A3) and (A4).

It is noteworthy that Lines and Jones's^{10,11} effective spin-Hamiltonian results in a j one-half our j value. Essentially their method is to minimize the free energy as we did in Sec. II, substitute the resulting Δ_{eq} into the expression for the total (exchange plus elastic) free energy, and then choose an effective Hamiltonian which yields the total free energy. The factor of $\frac{1}{2}$ difference in the " j " values arises from the Δ^2 term of the lattice free energy. When Δ_{eq} is substituted for Δ , this Δ^2 depends on $\langle\mathbf{A}\rangle^2$, and in the effective Hamiltonian it is of the form $\langle\mathbf{A}\rangle \mathbf{A}$. Their resulting effective Hamiltonian would be $\mathbf{A} - (\lambda^2\langle\mathbf{A}\rangle/2C)\mathbf{A}$.²² In earlier work, Rodbell and Owen,⁶ using a MFA, calculated the effective exchange energy and the distortion and isotropic contraction parameters for MnO and NiO in a manner similar to Lines and Jones,^{10,11} and therefore their work also reflects this factor of $\frac{1}{2}$.

²² The author has discussed this factor of $\frac{1}{2}$ with M. E. Lines and he concurs that the effective Hamiltonian used in this work is the appropriate one to use.